Protein Engineering, Design & Selection vol. 21 no. 12 pp. 709–720, 2008
Published online October 7, 2008 doi:10.1093/protein/gzn046

Rational stabilization of the C-LytA affinity tag by protein engineering

Víctor M. Hernández-Rocamora, Beatriz Maestro, Almudena Mollá-Morales[1] and Jesús M. Sanz[2]

Instituto de Biología Molecular y Celular, Universidad Miguel Hernández, Avda Universidad s/n, Elche 03202, Spain

[1]Present address: Instituto de Bioingeniería, Universidad Miguel Hernández, Avda Universidad s/n, Elche 03202, Spain.

[2]To whom correspondence should be addressed. E-mail: jmsanz@umh.es

The C-LytA protein constitutes the choline-binding module of the LytA amidase from *Streptococcus pneumoniae*. Owing to its affinity for choline and analogs, it is regularly used as an affinity tag for the purification of proteins in a single chromatographic step. In an attempt to build a robust variant against thermal denaturation, we have engineered several salt bridges on the protein surface. All the stabilizing mutations were pooled in a single variant, C-LytAm7, which contained seven changes: Y25K, F27K, M33E, N51K, S52K, T85K and T108K. The mutant displays a 7°C thermal stabilization compared with the wild-type form, together with a complete reversibility upon heating and a higher kinetic stability. Moreover, the accumulation of intermediates in the unfolding of C-LytA is virtually abolished for C-LytAm7. The differences in stability become more evident when the proteins are bound to a DEAE-cellulose affinity column, as most of wild-type C-LytA is denatured at ∼65°C, whereas C-LytAm7 may stand temperatures up to 90°C. Finally, the change in the isoelectric point of C-LytAm7 enhances its solubility at acidic pHs. Therefore, C-LytAm7 behaves as an improved affinity tag and supports the engineering of surface salt bridges as an effective approach for protein stabilization.

Keywords: affinity chromatography/choline-binding proteins/protein immobilization/protein stability/recombinant protein purification

Introduction

Proteins are intrinsically unstable molecules. Their stabilization energies typically range from 5–20 kcal mol^{-1}, and this value results from a delicate balance between two opposite forces—the stabilities of the folded and unfolded conformations—each in the order of 10^7 kcal mol^{-1} including covalent bonds (Baldwin and Eisenberg, 1987). This marginal stability allows an efficient turnover of proteins in the cell, where they are continuously synthetized and degraded depending on the cellular metabolic state. However, proteins have an enormous potential for industrial, biomedical and biotechnological processes (Kirk *et al.*, 2002) which, in many situations, would benefit from an enhancement in their stability: higher resistance to denaturation, better performance and durability in conditions far from standard (pH and ionic strength extremes, non-aqueous solvents), etc. In particular, thermoresistant proteins are suitable for their use in bioreactors at high temperatures, where the reaction rates are faster and the risk of microbial contamination is diminished (Vieille and Zeikus, 2001; Unsworth *et al.*, 2007). The determinants of thermostability on proteins have been thoroughly studied, especially from the structural comparison between homologous proteins from mesophillic and thermophillic organisms (Tanner *et al.*, 1996; Knapp *et al.*, 1997; Tahirov *et al.*, 1998; Maes *et al.*, 1999). However, there is no single, unequivocal molecular mechanism accounting for this thermostability, but a range of them occur in different proteins and organisms (Petsko, 2001; Vieille and Zeikus, 2001). This fact seriously complicates the modification of polypeptides by rational engineering procedures. Nevertheless, one of the most common mechanisms by which many proteins acquire their thermostability is the presence of surface ionic networks (Yip *et al*, 1995; Tanner *et al.*, 1996; Petsko, 2001; Vieille and Zeikus, 2001; Makhatadze *et al.*, 2003; Cheung *et al.*, 2005). The rationale behind is that a salt bridge will stabilize the protein if the energetic gain compensates the desolvation penalty arising from the elimination of the hydratation sphere of each ion. Since the dielectric constant of water decreases with temperature because of the increased thermal motion of water (Elcock, 1998), so does the desolvation penalty, and this results in a higher stability at high temperatures (Karshikoff and Ladenstein, 2001; Vieille and Zeikus, 2001). It also follows then that the formation of surface ionic networks, instead of separated salt bridges, is favored by the fact that the addition of a new charge to an already formed bond only requires the desolvation of that particular ion. This procedure currently constitutes one of the most promising ways of rationally thermostabilizing a protein (Loladze *et al.*, 1999; Pérez-Jiménez *et al.*, 2005; Strickler *et al.*, 2006) with the additional advantage that a surface mutation should indeed be, in general, less deleterious on the overall structure (and function) of the protein than a change inside the protein core (van den Burg and Eijsink, 2002).

Some biotechnological processes, such as protein purification by affinity chromatography or immobilization in a solid support, require the participation of the so-called affinity tags (Uhlen *et al.*, 1992; Waugh, 2005). Among these, the choline-binding modules (CBMs) (Pfam ID code PF01 473: http://www.sanger.ac.uk/cgi-bin/Pfam/getacc?PF01473) display a significant and specific affinity for choline and analogs. The major representative of the CBM family is C-LytA, the C-terminal module of the LytA autolysin from *Streptococcus pneumoniae*, which can be used as an affinity tag for specific immobilization of proteins in supports containing choline or derivatives such as DEAE-cellulose or amine-derivatized multiwell plates (Sanz *et al.*, 1988; Sánchez-Puelles *et al.*, 1992; Biomedal, 2004). Moreover, proteins fused to C-LytA can be single-step-purified upon elution from the column with an excess of choline (Ortega *et al.*, 1992; Ruíz-Echevarría *et al.*, 1995; Akerström *et al.*, 2000; Caubin *et al.*, 2001; Moldes *et al.*, 2004). Several properties makes it an attractive alternative to other immobilization/purification methods: (i) there are many simple, regenerable supports containing tertiary or

quaternary amines available; (ii) the optical transparency of buffers used in the purification procedure allows the direct quantification of protein content by UV absorption and its use in spectroscopical measurements; (iii) it is compatible with most buffers, including reducing reagents, EDTA, etc.; (iv) the degree of purity of preparations is very high, with the absence of persistent contaminants; and (v) the non-covalent, but strong, nature of C-LytA binding allows an easy regeneration of the matrix simply with extensive choline washes. The C-LytA polypeptide is a 135-aa repeat protein, built up from six conserved β-hairpins that configure four choline-binding sites (Fernández-Tornero *et al*., 2001). Every choline-binding site is configured by two aromatic residues from one hairpin and another one from the next, with the contribution of an additional hydrophobic side chain. The ligand is bound and stabilized presumably by hydrophobic and cation-π interactions. Calorimetric and spectroscopical analyses have demonstrated the presence of low-affinity and high-affinity choline-binding sites (Medrano *et al*., 1996; Usobiaga *et al*., 1996; Maestro and Sanz, 2005). Binding of choline promotes dimerization through the stacking of the last hairpin (Fernández-Tornero *et al*., 2001) and confers stability to C-LytA against thermal and chemical denaturation (Medrano *et al*., 1996; Maestro and Sanz, 2005). In contrast, the structure of the unligated form is not yet known. The analysis of the equilibrium unfolding of C-LytA induced by chemical reagents at neutral pH and room temperature has unveiled the accumulation of partly folded intermediates and a relevant structural independence between hairpins (Maestro and Sanz, 2005; Maestro and Sanz, 2007).

The ease of C-LytA purification, the knowledge about its stability, folding and spectroscopical characteristics, its reduced size and its wide biotechnological potential make this polypeptide a very attractive model to test current protein engineering procedures aimed at the improvement of its application as a robust affinity tag. Here, we describe the stabilization of C-LytA achieved by the creation of surface ionic interactions, leading to the C-LytAm7 protein. This variant represents a significative advance with respect to the wild-type form, i.e. a higher thermal stability and reversibility upon denaturation, and an enhanced purification yield in conditions far from standard (high temperatures and acidic pHs), that widens the application landscape of this protein. Besides these applications, this procedure may also pave the way for the rational design of more robust choline-binding peptidoglycan hydrolases specifically aimed to lyse *S. pneumoniae in vivo* (the so-called enzybiotics) (Nelson *et al*., 2001) that avoid denaturation at physiological temperatures.

Materials and methods

Materials

Guanidinium chloride (GdmCl) was purchased from Merck. Choline chloride and DEAE-cellulose were from Sigma. Owing to the hygroscopic properties of choline, concentrated stock solutions were always prepared from a freshly opened bottle and stored in aliquots at −20°C.

Site-directed mutagenesis

Mutagenesis to the 3′ moiety of the LytA gene coding for the C-LytA protein, contained in the pCE17 plasmid (Sánchez-Puelles *et al*., 1990), was carried out using the QuickChange Site-Directed Mutagenesis Kit (Stratagene, La Jolla, CA, USA) and the following oligonucleotide primers (introduced mutations are in boldface, and only one of the strands is shown):

5′-TCAATGGCACTTGG**AAA**TAC**AAA**GACAGTTCAGG-CTAT**GAA**CTTGCAGACCGCTGG-3′ (Y25K/F27K/M33E mutations, leading to pCE17rep1 plasmid);

5′-GGTACTGGTTCGAC**AAAAAA**GGCGAAATGGC-3′ (N51K/S52K mutations, pCE17rep2 plasmid);

5′-GGCGAAATGGCT**GAA**GGCTGGAAGAAAATCG-C-3′ (T57E mutation, pCE17rep3 plasmid);

5′-GGTCAAGTACAAGGAC**AAA**TGGTACTACTTAGA-CG-3′ (T85K mutation, pCE17rep4 plasmid);

5′-CCAGTCAGCGGACGGA**AAA**GGCTGGTACTACC-3′ (T108K mutation, pCE17rep5 plasmid);

5′-AATTCACAGTA**AAA**CCAGATGGCTTGATTAC-3′ (E128K mutation, pCE17rep6 plasmid), and

5′-GTAGAGCCAGATGGC**CGC**ATTACAGTAAAATA-A-3′ (L132R mutation, pCE17rep7 plasmid).

Protein purification

Wild-type and mutant C-LytA proteins were purified by affinity chromatography from the overproducing *Escherichia coli* strain RB791 harboring either the original pCE17 plasmid (Sánchez-Puelles *et al*., 1990) or its derivatives described earlier. Optimized materials and protocols contained in the C-LYTAG kit (Biomedal, Seville, Spain) were used. In order to remove the bound choline, the purified proteins were subsequently applied onto a HiTrap desalting column (1.6 × 2.5 cm) (GE Healthcare) at 20°C equilibrated in 20 mM sodium phosphate buffer, pH 7.0, plus 50 mM NaCl, and stored at −20°C. Protein concentration was determined spectrophotometrically as described previously (Sánchez-Puelles *et al*., 1990) using a molar absorption coefficient at 280 nm of 62 540 M^{-1} cm^{-1}.

Fluorescence spectroscopy

Fluorescence measurements were carried out on a PTI-QuantaMaster fluorimeter (Birmingham, NJ, USA), model QM-62 003SE, using a 5 × 5 mm path-length cuvette and a protein concentration of 6.3 μM. Tryptophan emission spectra were obtained using an excitation wavelength of 280 nm, with excitation and emission slits of 3 nm and a scan rate of 60 nm min^{-1}.

Circular dichroism spectroscopy

Circular dichroism (CD) experiments were carried out in a Jasco J-815 spectropolarimeter (Tokyo, Japan) equipped with a Peltier PTC-423S system. Isothermal wavelength spectra were acquired at a scan speed of 50 nm min^{-1} with a response time of 2 s and averaged over at least six scans at 20°C. Protein concentration was 6.3 μM and the cuvette path length was 1 or 2 mm. Buffers were 50 mM sodium phosphate (pH 6.0–8.0 and 12.5), 50 mM sodium acetate (pH 3.5–5.5) or 50 mM glycine (pH 2.5–3.0 and 9.0–10.7), plus the corresponding additions in each case. Final pH was measured *in situ* using a Crison Basic-20 pH-meter. Samples were centrifuged 5 min prior CD measuring. Ellipticities ($[\theta]$) are expressed in units of deg cm^2 $dmol^{-1}$, using the residue concentration of protein before centrifugation. For CD-monitored temperature-scanning denaturation experiments, the sample

was layered with mineral oil to avoid evaporation, and the heating rate was 60°C h^{-1}. When a second scan was required, the heated sample was cooled down in the same cuvette and left for at least 1 h for temperature equilibration. Since the transitions were not completely reversible in some cases, a thermodynamic analysis could not be carried out and the curves were only fitted to sigmoidal transitions in order to calculate the temperature midpoint (t_m). In order to measure the kinetic stability of proteins at high temperatures, aliquots of proteins were manually added to a previously thermostatted cuvette containing the corresponding buffer, mixed thoroughly and deposited back in the cell holder. This process, together with the necessary re-equilibration time, took ~20 s. Data after this dead time were fitted to a single exponential decay equation. For isothermal GdmCl titrations, aliquots from an 8.0 M denaturant stock solution were added stepwise and incubated for 5 min prior to recording the wavelength spectra. With GdmCl present, spectra could not be recorded below 215 nm owing to the high absorbance of the sample. Experiments were repeated at least three times.

Thermodynamic data analysis

Equilibrium chemical unfolding data were fitted by least squares to the corresponding two-state process according to Eq. (1) (Greene and Pace, 1974):

$$\Delta G = \Delta G_0 - m[\mathrm{GdmCl}] \quad (1)$$

where ΔG and ΔG^0 are the free energies of unfolding in the presence and absence of GdmCl, respectively, and m represents the dependence of ΔG with respect to the concentration of denaturant. The value of ΔG can be calculated as:

$$\Delta G = -RT \ln K_{eq} = -RT \ln \frac{[\theta]_I - [\theta]_X}{[\theta]_X - [\theta]_F} \quad (2)$$

where K_{eq} is the equilibrium constant between the initial and final states, $[\theta]_I$ and $[\theta]_F$ are the ellipticities of the initial and final state, respectively, and $[\theta]_X$ is the experimental ellipticity at a given GdmCl concentration. When required, a linear dependence of the $[\theta]_I$ and/or $[\theta]_F$ parametres with [GdmCl] was implemented in Eq. (2) for a better fitting of sloping pre- and/or post-transitional baselines.

Equilibrium thermal unfolding data were fitted by least squares to the corresponding two-state process according to the Gibbs–Helmholtz equation:

$$\Delta G = \Delta H_m \left(1 - \frac{T}{T_m}\right) - \Delta C_p \left[(T_m - T) + T \ln \frac{T}{T_m}\right] \quad (3)$$

where ΔH_m is the van't Hoff enthalpy, T_m is the midpoint of denaturation (in Kelvin) and ΔC_p is the difference in heat capacity between the native and denatured states.

To analyze data involving the denaturation of dimeric species, we employed a modified form of Eq. (3) (Backmann *et al*., 1998) to take into account the concentration of the protein:

$$\Delta G = \Delta H_m \left(1 - \frac{T}{T_m}\right) - \Delta C_p \left[(T_m - T) + T \ln \frac{T}{T_m}\right] - RT \ln(2P_t) \quad (4)$$

where P_t denotes the total concentration of protein dimers.

For the estimation of ΔC_p as deduced from the increment in accessible surface area (ΔASA) upon denaturation, the following procedure was used. First, a three-dimensional model of C-LytAm7 was obtained from the PDB file that contains the structure of C-LytA bound to choline (PDB code 1HCX) (Fernández-Tornero *et al*., 2001). The seven mutations leading to C-LytAm7 were introduced, and the resulting structure was energy-minimized using the SwissPDBViewer v3.7 utilities (Guex and Peitsch, 1997). Moreover, a model for the unfolded protein was obtained by assigning β-sheet-extended dihedral angles to the whole polypeptide chain. The ASA of the resulting structures was calculated using the program ASAcalc (Freire *et al*., 1997), which is based on the Lee and Richards algorithm (Lee and Richards, 1971). Calculations were done using a solvent radius of 1.4 Å and a slice width of 1.25 Å. Results are averaged over 12 rotations. ASAcalc provided polar and non-polar accessible surface areas (ASA(p) and ASA(np), respectively). ΔC_p was then estimated according to Myers *et al*. (1995):

$$\Delta C_p = 0.28 \cdot \Delta\mathrm{ASA(np)} - 0.09 \cdot \Delta\mathrm{ASA(p)} \quad (5)$$

On-column thermal stability of C-LytA

Samples of 1 mg of desalted C-LytA or C-LytAm7 proteins were added to Eppendorf tubes containing 1 ml of DEAE-cellulose equilibrated in phosphate buffer (pH 7.0) plus 150 mM NaCl and incubated at 20°C for 30 min. After a 5 min centrifugation step (13 000*g*), the supernatant was removed, and the resin was washed twice with equilibration buffer. The tubes were subsequently incubated at a determined temperature for 30 min, followed by equilibration at 20°C for at least 10 min. After a 5 min centrifugation step (13 000*g*), the supernatant was removed, and the resin was washed twice with phosphate buffer in order to remove denatured protein released from the resin. Finally, the support was incubated for 5 min with 1.5 ml of phosphate buffer (pH 7.0) plus 150 mM choline to specifically elute the bound (folded) protein. In some experiments, the equilibration step at room temperature was omitted and the elution step was carried out at high temperature. Eluted samples were spectroscopically quantified and compared with the control incubated at 20°C throughout the whole process.

Results and discussion

Design of mutations

In order to engineer new electrostatic interactions on the surface of C-LytA, we restricted the changes to residues that, according to the structure of the ligand-bound protein (Fernández-Tornero *et al*., 2001), should not substantially affect neither the overall packing nor the dimerization region or the choline-binding sites. The following mutations were selected (Fig. 1):

Y25K/F27K/M33E These three positions are located in the β-strands of the first hairpin. They face the N-terminal region and are not involved in packing. Glu-18 and Glu-54 (in loop 3) flank this triad. Mutations might help create a five-residue ionic network in which Lys-27 interacts with Glu-18 and Glu-33, and Lys-25 would be surrounded by Glu-18, Glu-33 and Glu-54 (Fig. 1A).

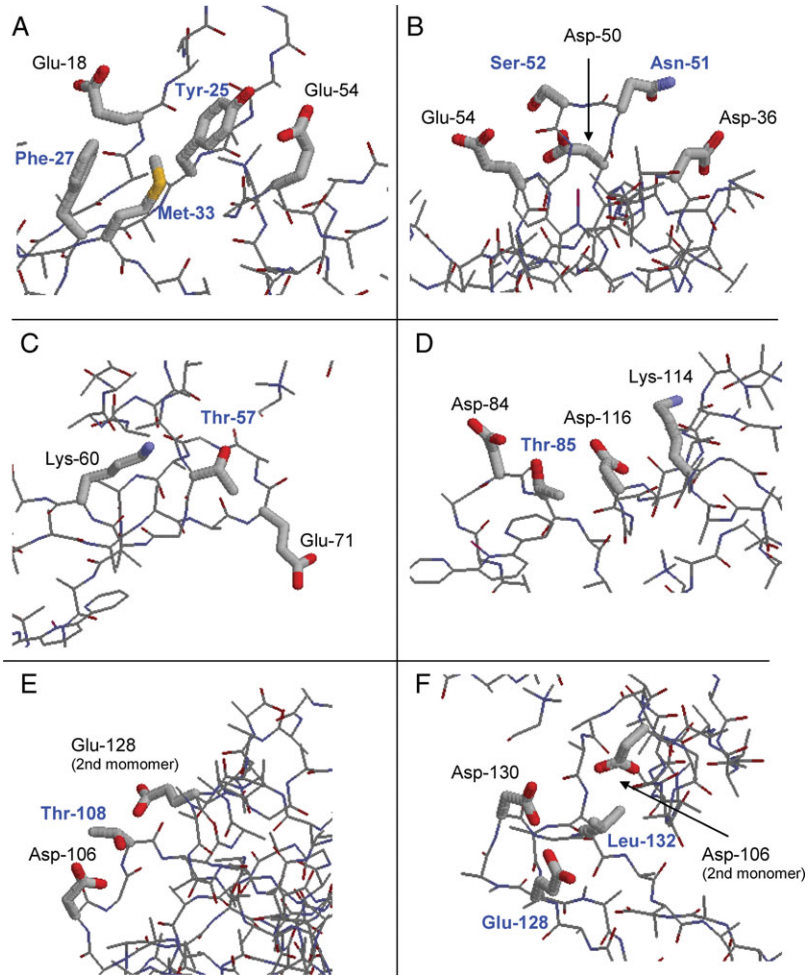

Fig. 1. Design of mutations based on the structure of choline-bound C-LytA (PDB code 1HCX). Relevant residues are highlighted in thick wireframe representation. Mutated positions are labeled in bold and blue. Figures were rendered with RASMOL (Bernstein, 2000).

N51K/S52K Asn-51 and Ser-52, in loop 3, are in close proximity to an acidic alineation of Asp-36 (hairpin 2), Asp-50 and Glu-54 (loop 3). Incorporation of basic side chains could also configure a five-residue ion network (Fig. 1B).

T57E A favorable electrostatic interaction with Lys-60 (hairpin 3) can be envisaged upon changing Thr-57 (hairpin 3) into glutamate. Although Glu-71 (loop 4) is also close to Thr-57, its side chain is, in principle, pointing away to the solvent (Fig. 1C).

T85K The favorable contact of Lys-114 with Asp-116 (loop 6) may be extended to Asp-84 (in the β-turn of hairpin 4) provided that Thr-85 is changed to a basic residue, and thus promoting a four-residue ionic association (Fig. 1D).

T108K Thr108 is located in the β-turn of hairpin 5, near Asp-106, and therefore it was chosen for the incorporation of a lysine residue. Moreover, after the dimerization triggered by choline, the Glu-128 residue on the second monomer (hairpin 6) might complete a three-residue network (Fig. 1E).

E128K AND L132R The dimerization surface of C-LytA is not completely hydrophobic but involves the participation of polar or even charged residues. Among these, Glu-128, Asp-130 and Asp-106 (second monomer) surround Leu-132, very close to the C-terminus of the protein, creating an acidic environment that might be stabilized by the incorporation of basic residues either in the 128 or in the 132 positions (Fig. 1F).

Thermal stability of mutants

Mutations were introduced in the C-LytA protein by PCR-based site-directed mutagenesis on the pCE17 vector. Next, all mutants were overexpressed and single-step-purified in DEAE-cellulose as described for the wild-type protein (see Materials and Methods), with similar yields. This demonstrated that the mutants are well folded and active, as their ability to recognize choline was not affected as a consequence of mutations. Figure 2A displays the intrinsic fluorescence spectrum of wild-type C-LytA, with a maximum centered at 333 nm. We chose to check the effect of 10 mM choline, since this is sufficient to occupy to a large extent both high- and low-affinity sites (92 and 72%, respectively) (Medrano *et al.*, 1996), and because it constitutes the threshold concentration above which C-LytA is eluted from a DEAE-cellulose column (Maestro *et al.*, 2007). Moreover, the strong stabilization induced by higher ligand concentrations after saturation of the low-affinity sites might somehow mask the intrinsic stability of the proteins.

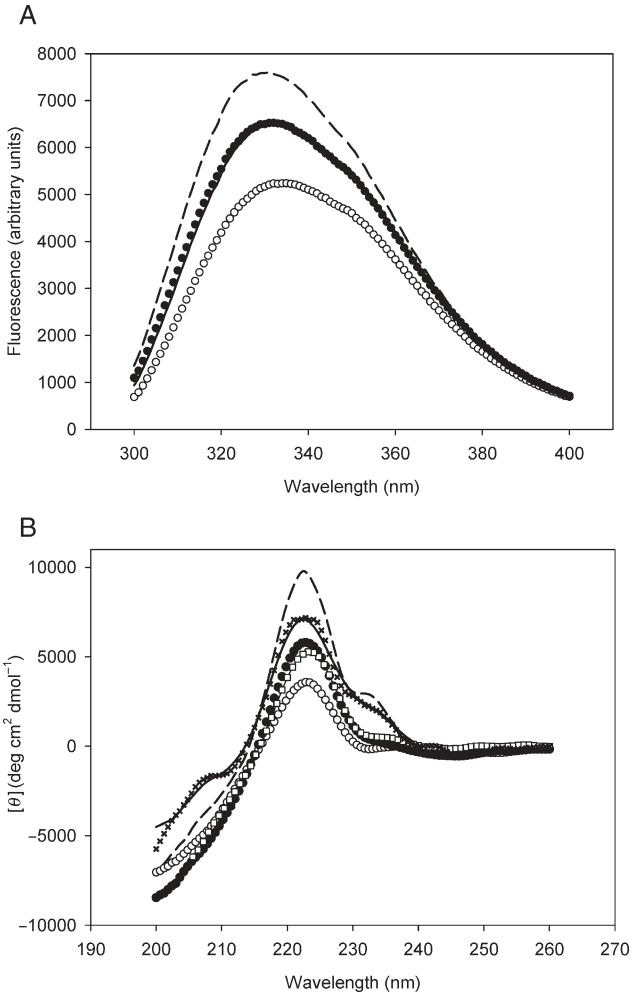

Fig. 2. Spectroscopical characteristics of C-LytA and C-LytAm7 proteins. (A) Intrinsic fluorescence spectra of C-LytA (solid line), C-LytA in the presence of 10 mM choline (dashed line), C-LytAm7 (open circle) and C-LytAm7 in the presence of 10 mM choline (filled circle). (B) Far-UV CD. Same scheme as in (A), plus C-LytA and C-LytAm7 in the presence of 500 mM NaCl (cross and open box, respectively).

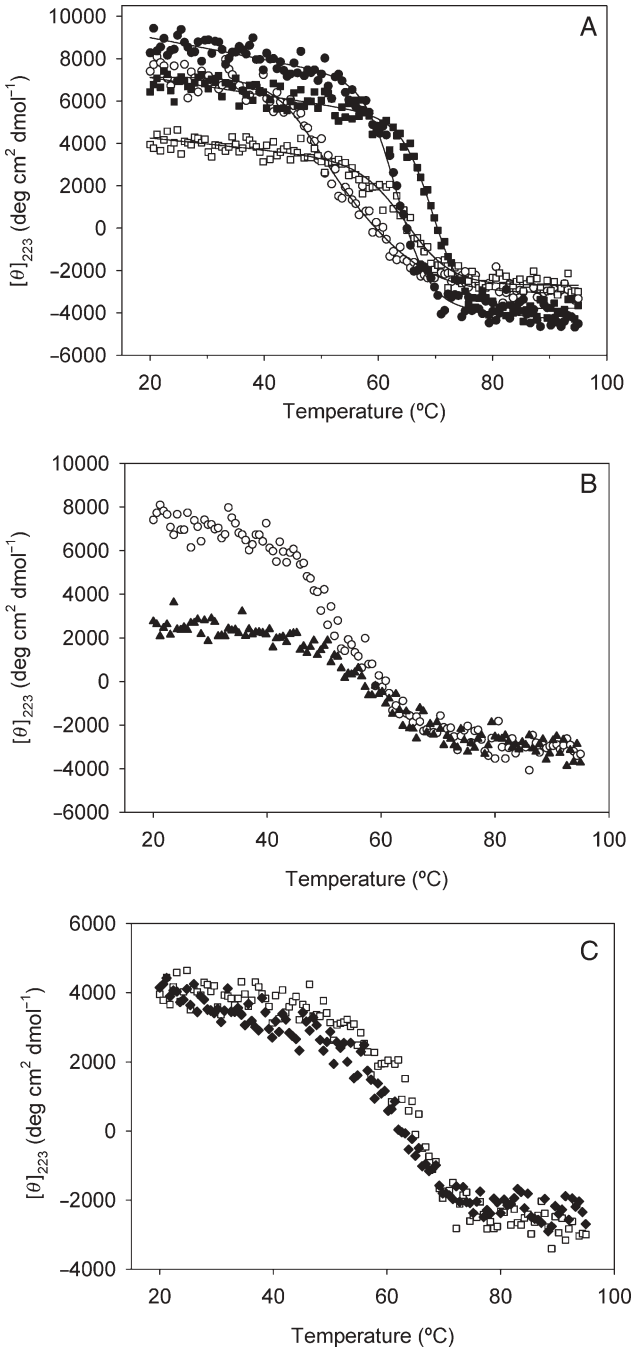

Fig. 3. Thermal stability of C-LytA and C-LytAm7 monitored by far-UV CD. (A) Thermal scans of C-LytA in the absence (open circle) and presence of 10 mM choline (filled circle), and of C-LytAm7 in the absence (open box) and presence of 10 mM choline (filled box). Data were fitted to a simple sigmoidal equation except C-LytA in the absence of choline, where a double, consecutive sigmoidal equation was used. (B) Reversibility of the thermal unfolding of C-LytA: open circle, first scan; filled triangle, second scan. (C) Reversibility of the thermal unfolding of C-LytAm7: open box, first scan; filled diamond, second scan.

As depicted in Fig. 2A, the addition of 10 mM choline shifts the maximum of the intrinsic fluorescence spectrum to 328 nm and increases its intensity, which is compatible with the tryptophan residues in the binding sites being buried upon the addition of the ligand (Fernández-Tornero *et al*., 2001; Maestro and Sanz, 2005). On the other hand, the far-UV CD spectrum of the protein, which does not reflect the actual content in secondary structure owing to intense aromatic contributions (Sánchez-Puelles *et al*., 1990; Medrano *et al*., 1996), also detects choline binding through the enhancement of the positive bands in the 220–235 nm region and the sharpening of the shoulder centered at 233 nm (Fig. 2B).

Measurement of CD signal at 223 nm has been used in the past to assess the thermal stability of C-LytA (Usobiaga *et al*., 1996; Maestro and Sanz, 2005). Denaturation of the wild-type form in the absence of choline is a two-phase process (Fig. 3A), with the accumulation of an intermediate (I_1) at ~55°C that has been described as having the first β-hairpin unfolded, while maintaining the majority of the protein intact (Maestro and Sanz, 2005). The appearance of I_1 is an irreversible, not very reproducible process that leads to its accumulation as the predominant species upon cooling down the sample. Consequently, a rescan only yields the second transition, which solely accounts for the stability of the I_1 form (Maestro and Sanz, 2005) (Fig. 3B). The denaturation midpoint (t_m) of the second thermal transition was 61.0°C, in good agreement with previous results (Usobiaga *et al*., 1996; Maestro and Sanz, 2005). The thermal stability of the mutants was checked with the same procedure (Table I). No thermodynamic analysis was attempted, as the thermal denaturation of

Table I. Thermal stability of C-LytA mutants

Mutant	t_m (°C) (no choline)	Δt_m^a (°C) (no choline)	t_m (°C) (10 mM choline)	Δt_m^a (°C) (10 mM choline)
Wild-type	61.0 ± 1.1	—	62.5 ± 1.3	—
Y25K/F27K/M33E	62.6 ± 0.2	1.6	62.7 ± 0.4	0.2
N51K/S52K	63.3 ± 0.2	2.3	63.1 ± 0.9	0.6
T57E	51.7 ± 1.1	−9.3	57.9 ± 0.2	−4.6
T85K	60.0 ± 0.5	−1.0	66.0 ± 0.4	3.5
T108K	60.2 ± 1.0	−0.8	64.9 ± 0.7	2.4
E128K	54.7 ± 0.4	−6.3	60.8 ± 0.4	−1.7
L132R	55.1 ± 0.6	−5.9	63.6 ± 0.5	1.1
Y25K/F27K/M33E/ N51K/S52K/T85K/ T108K (C-LytAm7)	65.1 ± 0.3	4.1	69.6 ± 0.2	7.1

[a]$\Delta t_m = t_m(\text{mutant}) - t_m(\text{wild-type})$.

C-LytA is a complex process involving metastable intermediates and protein aggregation (Usobiaga *et al*., 1996; Maestro and Sanz, 2005). On the other hand, with 10 mM choline present, both wild-type (Fig. 3A) and the mutants (not shown) presented a single transition owing to the destabilization of the I_1 intermediate (Maestro and Sanz, 2005). Results of all the fittings are shown in Table I. Compared with the wild-type protein, mutants Y25K/F27K/M33E and N51K/S52K displayed a moderate but reproducible stabilization of the non-ligated form. These mutations are located in the N-terminal part of the protein and help to stabilize this rather loosely packed region (Maestro and Sanz, 2005). Conversely, both T85K and T108K mutants showed stabilization only in the presence of choline. These changes are located in the C-terminal part of the protein, which is more sensitive to choline binding, as it contains the ligand-triggered dimerization region (Fernández-Tornero *et al*., 2001), and it is likely that the new interactions created in these variants may require the integrity of the dimer to be effective. In fact, the T108K-mediated network can only be accomplished once the dimer is formed, as it needs the participation of residues from the two monomers (Fig. 1E). This idea receives more support when analyzing the E128K and L132R mutants. Here, the amino acid changes turned out to be highly destabilizing for the free protein, whereas no strongly adverse effects were found in the presence of choline (Table I). In the absence of ligand, and therefore, of dimerization, the introduction of voluminous lysine and arginine in the cited positions may lead to a destabilizing steric hindrance interactions in the last β-hairpin. On the other hand, the choline-induced dimerization would bring along the rest of the residues needed to create the ionic networks devised in Fig. 1F, therefore overcoming the destabilizations cited above (Table I). In any case, these results suggest that the dimerization region is not suitable for introducing new salt bridges. Finally, among all mutations tested, the T57E change turned out to be the most destabilizing, with a decrease of more than 9°C in the t_m of the ligand-free form (Table I). This suggests that the possible repulsion with Glu-71 overcomes any favorable interaction with Lys-60 (Fig. 1).

Construction and stability analysis of the multiple mutant C-LytAm7

The next step was to combine all mutations that meant a noticeable stabilization in either the ligand-free or the ligand-bound forms of C-LytA. This was carried out by sequential site-directed mutagenesis of the pCE17 vector (see Materials and methods), which yielded the pCE17m7 plasmid that overexpressed the multiple C-LytAm7 mutant. This C-LytA variant contained seven changes, namely Y25K, F27K, M33E, N51K, S52K, T85K and T108K. The C-LytAm7 protein was purified in a good yield with the standard affinity chromatography procedure employed with the wild-type and the partial mutants, demonstrating that its ability to recognize choline or choline analogs was unaffected. The initial characterization of C-LytAm7 was assessed by spectroscopy. Figure 2A shows that the intrinsic fluorescence spectrum of the mutant is slightly red-shifted and has a decreased intensity compared with that of the wild-type form. These differences are maintained in the presence of 10 mM choline. Moreover, the far-UV CD spectrum is also somewhat different to that of the C-LytA module, displaying an overall decreased intensity and a less evident 233 nm-centered shoulder even in the presence of choline (Fig. 2B). Nevertheless, we believe that these changes do not necessarily reflect a high conformational change compared with the wild-type protein. C-LytA is a relatively small protein with a high aromatic content (12 tryptophans out of 135 residues), so that any structural technique monitoring the environment of the aromatic side chains (like fluorescence or CD in this case) should be very sensitive to subtle conformational rearrangements. For example, three of the mutated positions (Asn-51, Thr-85 and Thr-108) are in close proximity to Trp-48, Trp-86 and Trp-110, respectively (Fernández-Tornero *et al*., 2001). This hypothesis is reinforced by the fact that a mere increase in ionic strength induces in the C-LytAm7 variant an intensity enhancement of 30% of the CD bands mainly related to aromatic contributions, whereas the spectrum of the wild-type remains unaltered (Fig. 2B).

The thermal stability of C-LytAm7 was assessed by CD-monitored thermal scans. In contrast to the wild-type protein, the mutant displayed a single thermal transition as shown in Fig. 3A. This, together with the full reversibility displayed by performing a second scan on the same sample (Fig. 3C) after a 30 min incubation at high temperatures, suggested the lack of accumulation of the I_1 intermediate even in the absence of choline. As expected, C-LytAm7 turned out to be more thermostable than wild-type C-LytA (Fig. 3A, Table I). The stabilization acquired upon mutation is more evident in the presence of 10 mM choline (7.1°C) than in its absence (4.1°C). It should be reminded that the mutations were designed on the basis of the choline-bound structure of C-LytA, as the structure of the free protein is not yet known. For this reason, the conformational effects occurring in the ligand-free form are less predictable. On the other hand, the relative stability of the mutant compared with the wild-type form was maintained in an excess of choline (150 mM) (data not shown).

To check the actual contribution of electrostatic forces to the stability of C-LytAm7, thermal scans were carried out in the presence of 500 mM NaCl. Data are shown in Table II. Within error, the t_m of the wild-type C-LytA protein was not substantially affected by salt (Table II), either in the presence or in the absence of choline. In contrast, ionic strength induced in C-LytAm7 a destabilization of around 2–3 degrees (Table II), confirming the important role of

Table II. Effect of ionic strength on the thermal stability of C-LytA variants

Protein	[Choline] (mM)	t_m (in 50 mM NaCl) (°C)	t_m (in 500 mM NaCl) (°C)	Δt_m[a] (°C)
Wild-type	0	61.0 ± 1.1	62.5 ± 1.3	1.5
	10	62.5 ± 1.3	62.3 ± 0.1	−0.2
C-LytAm7	0	65.1 ± 0.3	62.4 ± 0.3	−2.7
	10	69.6 ± 0.2	67.7 ± 0.2	−1.9

[a]$\Delta t_m = t_m$ (in 500 mM NaCl) − t_m (in 50 mM NaCl).

electrostatic interactions. In fact, the addition of 500 mM NaCl decreased the stability of unligated C-LytAm7 to the same levels as the wild-type, whereas the choline-bound form still retained a higher t_m (Table II). This again indicates that the design of thermostability is more robust when the choline-bound species are taken into account.

The 4–7 degree stabilization mentioned above was achieved by the concerted action of up to seven mutations. This can be deemed as only moderate taking into account the number of mutations involved, but the cases in which a single mutation introduced by site-directed mutagenesis induces a remarkable thermostabilization are not frequent in the literature. In fact, the accumulation of several low-energy changes distributed throughout the sequence is a natural, common mechanism for the stabilization of proteins from thermophillic organisms (Numata *et al*, 1995; Petsko, 2001). In any case, one possible explanation for this result lies on the strongly directional nature of salt-bridge interactions. In this sense, Iqbalsyah and Doig (2005) have reported the non-expected lack of stabilization of a salt bridge upon the addition of a third group with the aim of forming a Glu–Lys–Glu triad in an α-helical peptide. The authors attributed this effect to the inability of the central Lys to form two salt bridges simultaneously. It is probable that, in our case, some of the central residues located within networks, especially those involving many groups such as that formed upon the Y25K/F27K/M33E triple mutation (Fig. 1A), cannot reach the adequate positioning of their side chains so as to satisfy simultaneous electrostatic interactions, thus hampering the necessary cooperativity.

Folding thermodynamics

We studied the folding thermodynamics of the wild type C-LytA and the C-LytAm7 mutant protein using GdmCl. The use of the weaker, non-ionic denaturant urea was discarded, as it only leads at the highest concentrations to a partial, incomplete denaturation of C-LytA (data not shown). The chemical denaturation scheme of monomeric, unligated wild-type C-LytA by GdmCl at 20°C involves the accumulation of the I_1 intermediate at ~2.0 M denaturant and a second intermediate (I_2) with residual structure even at the highest guanidinium concentrations (7.4 M) (Maestro and Sanz, 2005) (Fig. 4C). Since I_1 builds up from the partial unfolding of secondary structure without affecting the location of tryptophan residues (Maestro and Sanz, 2005), the ellipticity at 219 nm (which mainly reports changes in β-structure) substantially decreases in the 0–2 M denaturant range, whereas the signal at 226 nm (a probe of tryptophan environment) barely changes (Fig. 4A and B) (Maestro and Sanz, 2005). That is, the CD-monitored titration curves are highly dependent on the wavelength used. In contrast, the I_1 intermediate cannot be detected in the case of C-LytAm7, as the two curves are coincident in the same GdmCl range (Fig. 4A and B, Table III). This is also in agreement with the thermal unfolding data shown in Fig. 3 and discussed above. Moreover, the residual CD spectrum ascribed to the I_2 intermediate is indistinguishable from that of the wild-type protein (Fig. 4C). With respect to the curve obtained at 226 nm for C-LytAm7 (and, to a lesser degree, at 219 nm), there is a sloping, pre-transitional baseline that should not be attributed to a conformational change but rather to a less specific effect on the spectrum owing to the ionic strength supplied by GdmCl (Fig. 2B) (see below). In fact, the values of $[\theta]_{226}$ obtained in the presence of 2 M NaCl or 2 M GdmCl are very close (Fig. 4B).

The titrations obtained at 20°C and at 226 nm were fitted to a two-state denaturation model by a linear extrapolation method. Results are shown in Table III. Data for C-LytA are in accordance with those described before (Maestro and Sanz, 2005); the $I_1 \rightarrow I_2$ transition was monitored, as the $N \rightarrow I_1$ change is non-cooperative and contributes little to the unfolding energetics. On the other hand, the calculated thermodynamic stability of unligated C-LytAm7 at 20°C is of the same magnitude as the wild-type form, irrespective of its thermostability (Table I). Similar results were obtained upon fitting the 219 nm data (Fig. 1A, Table III), ruling out the accumulation of I_1 in significant amounts. It can be argued that the high ionic strength contributed by GdmCl might be a source of instability, screening the favorable engineered charge–charge interactions and reducing the stability of unligated C-LytAm7 to the wild-type levels as deduced from thermal scans (Table II). To check this point, and taking advantage of the thermal reversibility shown in Fig. 3C for the C-LytAm7 mutant, we calculated ΔG for this protein by thermal denaturation experiments at different pHs, carrying out a van't Hoff analysis of the resulting thermograms. This procedure would allow the calculation of folding energetics without the interference of possible ionic strength effects caused by GdmCl. Figure 5A shows the thermal denaturation profiles of C-LytAm7 at several pHs. In all cases, a single sigmoidal, reversible transition could be seen, which was fitted to the Gibbs–Helmholtz equation [Eq. (3)]. Since ΔC_p is unknown for C-LytA, we used two different approaches in order to calculate the T_m's and van't Hoff enthalpies (ΔH_m) from the thermograms. In one case, we assumed the effect of ΔC_p on the enthalpy of unfolding to be negligible over the transition region (Swint and Robertson, 1993). On the other hand, it has been thoroughly studied for many proteins the dependence of ΔC_p as a function of the increment in accesible surface area upon unfolding (ΔASA) (Myers *et al*., 1995). As the three-dimensional structure of choline-unligated C-LytA or C-LytAm7 is unknown, we chose one monomer from the published structure of the dimeric choline-bound C-LytA (Fernández-Tornero *et al.*, 2001) to estimate a ΔASA value (and therefore the theoretical ΔC_p) as described in the Materials and Methods section [Eq. (5)]. This approach yielded a value of 5012.84 Å^2 for non-polar ΔASA and 3494.50 Å^2 for polar ΔASA, leading to an estimate of ΔC_p of 1.04 kcal mol^{-1} K^{-1}. However, it should be pointed out that this estimation may constitute the maximum limit of the real value, as the structure of the non-ligated protein may be looser than the choline-bound species

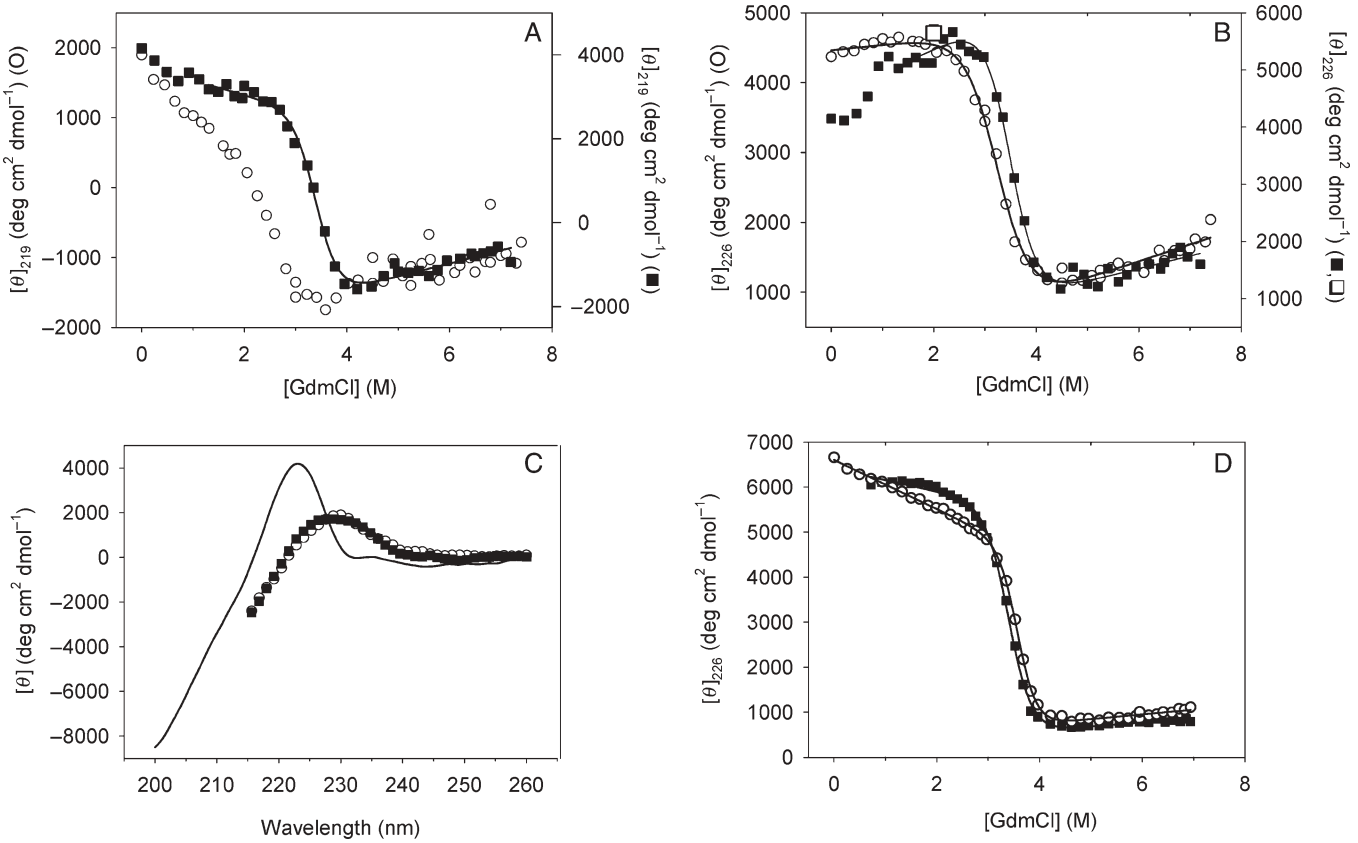

Fig. 4. Equilibrium unfolding by GdmCl monitored by far-UV CD. (A) Titration of the ellipticity at 219 nm: open circle, C-LytA; filled box, C-LytAm7. A double *Y*-axis has been drawn for clarity purposes. Solid line indicates the fitting to Eq. (2) for C-LytAm7. Data between 0 and 1.5 M GdmCl were not included in the fitting owing to unspecific salt effects described in the text that preclude the integration of a reliable pre-transitional baseline in the equation. (B) Titration of the ellipticity at 226 nm. Same symbol scheme as above. Solid lines indicate the fittings to Eq. (2). Data for C-LytAm7 between 0 and 1.5 M GdmCl were not included in the fitting as in (A). (C) Wavelength spectrum of C-LytAm7 in 0 M (solid line) and 7.0 M GdmCl (filled circle), and of C-LytA in 7.0 M GdmCl (open circle). (D) Titration of the ellipticity at 226 nm in the presence of 10 mM choline: open circle, C-LytA; filled box, C-LytAm7. Solid lines indicate the fittings to Eq. (2).

Table III. Thermodynamical stability of C-LytA and C-LytAm7

Conditions	Protein	Transition monitored	Unfolding parameters[a]		
			m (kcal mol^{-1} M^{-1})	[GdmCl]$_{1/2}$ (M)	ΔG (kcal mol^{-1})
No choline	C-LytA	$I_1 \rightarrow I_2$	2.1 ± 0.1	3.3 ± 0.1	6.9 ± 0.1
	C-LytAm7	$N \rightarrow I_2$	2.1 ± 0.1	3.4 ± 0.1	7.1 ± 0.1
	C-LytAm7	$N \rightarrow I_2$[b]	2.2 ± 0.1	3.3 ± 0.1	7.3 ± 0.1
10 mM choline	C-LytA	N_2•ch→$(I_2)_2$•ch[c]	3.1 ± 0.2	3.5 ± 0.1	10.9 ± 0.2
	C-LytAm7	N_2•ch→$(I_2)_2$•ch[c]	2.6 ± 0.2	3.5 ± 0.1	9.1 ± 0.2

[a]Data obtained applying Eqs (1) and (2).
[b]Transition monitored at 219 nm.
[c]'•ch' denotes choline-saturated species.

(Maestro and Sanz, 2005) and therefore the ΔASA values are also probably lower. In any case, we did not observe any substantial difference in calculating ΔH_m and T_m from the temperature-scan experiments using either estimate of ΔC_p (data not shown). Figure 5B shows the dependence of t_m on pH. The melting temperature remained constant in the pH interval 5.5–9.1 and decreased outside these limits. Remarkably, the van't Hoff enthalpies do not show a clear trend in the whole pH range tested (2.2–10.7), and consequently we were unable to calculate a reliable value of ΔC_p from the slope of the plot of ΔH_m versus T_m (Swint and Robertson, 1993) (Fig. 5C). A possible reason for this phenomenon is that the ΔC_p value for C-LytAm7 is indeed very low and points to entropic effects as the main responsible factor for C-LytAm7 thermal denaturation. Finally, Fig. 5D displays the maximum and minimum estimations of ΔG at 20°C for the C-LytAm7 protein as a function of pH, employing Eq. (3) and making use of ΔC_p values of 0 and 1.04 kcal mol^{-1} K^{-1}, respectively. In any case, the stability of the protein is maximal at pH's near neutrality, confirming that under these conditions the distribution of charges in the protein is optimal. Moreover, this approach may serve to

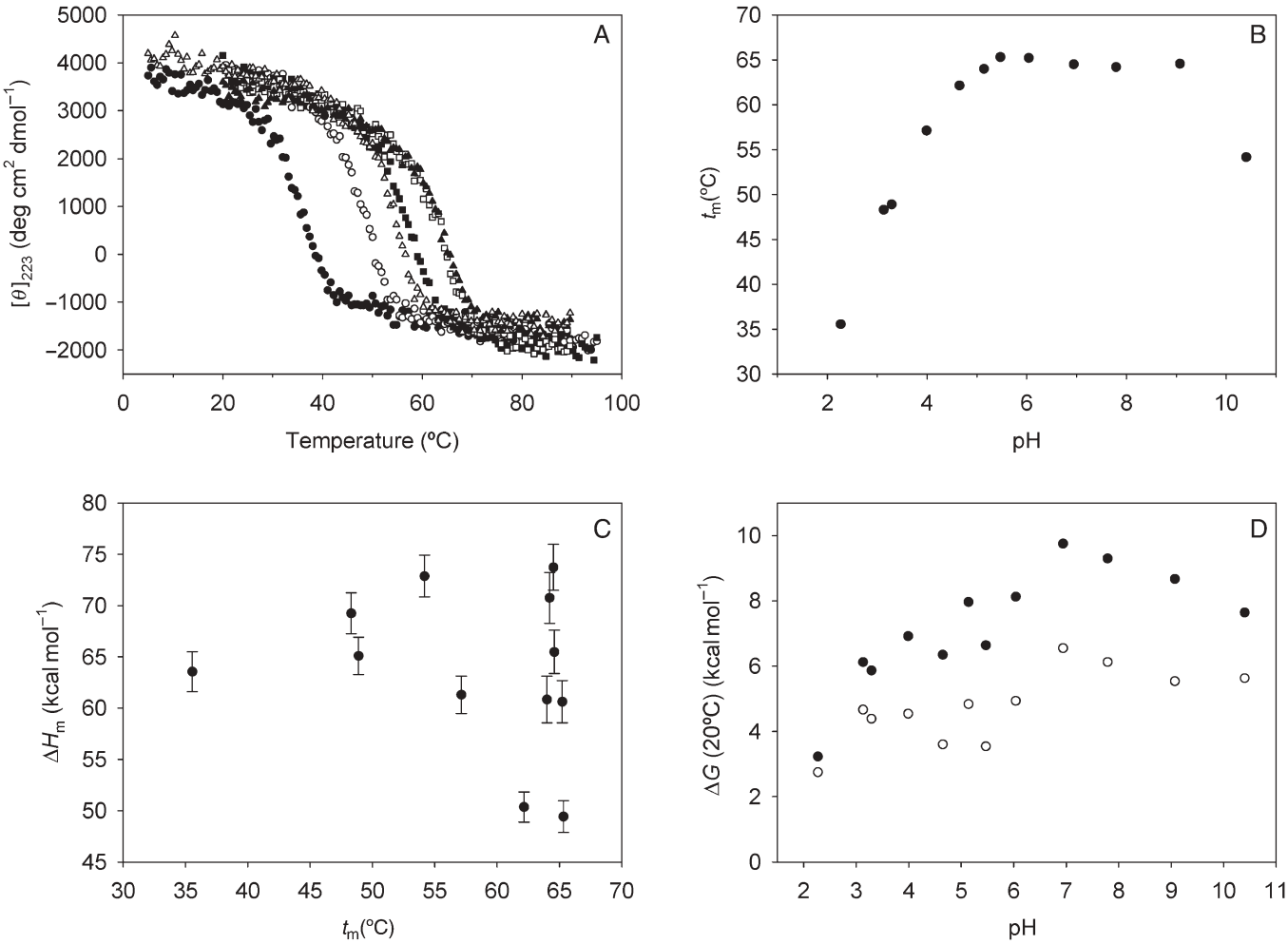

Fig. 5. Effect of pH on the equilibrium thermal unfolding of C-LytAm7. (A) Some representative temperature scans of C-LytAm7 performed at pH 2.2 (filled circle), 3.1 (open circle), 4.0 (filled box), 5.1 (open box) and 7.8 (filled triangle). (B) Dependence of t_m (in Celsius), calculated from van't Hoff analysis of C-LytAm7 thermograms, as a function of pH. Error bars are smaller than symbol size and are not represented. (C) Dependence of van't Hoff enthalpy (ΔH_m) with t_m. (D) Estimation of the upper and lower limits of ΔG (20°C) as a function of pH, calculated using Eq. (3) and employing $\Delta C_p = 1.04$ kcal mol^{-1} K^{-1} (open circle) or $\Delta C_p = 0$ kcal mol^{-1} K^{-1} (filled circle).

determine ΔG at pH 7.0 and 20°C and compare it with the values obtained with GdmCl (Table III). As described above, GdmCl denaturation of C-LytA and C-LytAm7 at 20°C is incomplete, leading to an intermediate (I_2) with residual structure (Fig. 4C) (Maestro and Sanz, 2005). For the wild-type protein, nevertheless, complete denaturation can be achieved by SDS, and this has allowed us to calculate the free energy associated to full unfolding, yielding a value of $\Delta G = 9.9$ kcal mol^{-1} (Maestro and Sanz, 2007). This value is precisely in the upper limit of ΔG estimation for C-LytAm7 from thermal data (Fig. 5D), assuming that ΔC_p is very low (Fig. 5C). Therefore, we believe that the stability of C-LytAm7 is certainly very close to that of wild-type C-LytA at 20°C and that any possible masking effect of the ionic strength contributed by GdmCl does not affect the stability calculations shown in Table III that are achieved upon linear extrapolation back to 0 M denaturant (and to 0 M ionic strength). It is also likely that salt effects are only effective at higher temperatures than 20°C.

Even in the presence of 10 mM choline, which makes salt screening effects less evident at high temperatures (Table II), the folding energetics of the wild-type and mutant proteins are still rather similar at 20°C (Fig. 4D, Table III). Likewise, we fitted the thermograms shown in Fig. 3A for both C-LytA and C-LytAm7 in 10 mM choline to the modified Gibbs–Helmholtz equation [Eq. (4)], which takes into account the dimeric nature of the proteins in the presence of the ligand. Despite the thermal stabilization caused by the ligand (Table II), the ΔH_m values were of similar magnitude as those of unligated proteins (76.9 ± 2.4 kcal mol^{-1} for C-LytA, 79.9 ± 1.4 kcal mol^{-1} for C-LytAm7) that add more evidence in favor of a very low ΔC_p for these polypeptides. The estimated ΔG values at 20°C depend too strongly on the value of ΔC_p and, in the absence of a reliable calculation of this parameter, they are therefore not shown. However, irrespective of the ΔC_p chosen, we found that the predicted values of $\Delta\Delta G$ for both proteins ($\Delta G_{wild\text{-}type} - \Delta G_{mutant}$) lie within a range of ± 1 kcal mol^{-1} and reinforce the energetic similarities between the two proteins at 20°C.

The results shown so far point to the hypothesis that C-LytAm7 displays its acquired stability only at temperatures >20°C. This is expected from theory, since as stated above, the desolvation penalty for ionic residues establishing an interaction decreases with temperature (Elcock, 1998). One way to check this hypothesis would be to perform the chemical denaturations at high temperatures, but wild-type C-LytA

undergoes conformational transitions at temperatures >40°C, leading to the accumulation of intermediates that could excessively complicate the equilibrium analysis (Usobiaga *et al*., 1996). Instead, we measured the kinetic stability of the proteins at temperatures above their t_m's. Temperatures of 70°C and 80°C were chosen to carry out the experiments in the absence and presence of 10 mM choline, respectively. As depicted in Fig. 6, the C-LytAm7 mutant is in all cases kinetically more stable than C-LytA. The manual mixing procedure precluded the reliable analysis of the approximately first 20 s of the experiment. Therefore, we fitted the rest of the time trace to a single exponential in order to have an idea of the kinetics involved. Data of these fittings are depicted in Table IV and show that the C-LytAm7 mutant unfolds in solution at roughly half the rate than the wild-type form. Although this result cannot be used as a criterion for inferring thermodynamic stabilities (particularly as wild-type C-LytA undergoes an irreversible step leading to the I_1 intermediate), we believe that it can be taken as an indirect evidence of the superior thermostability of the mutant protein.

Performance of C-LytAm7 as affinity tag in protein immobilization procedures

Effect of temperature The mutations incorporated on C-LytAm7 might lead to an improved affinity tag to be employed in biotechnological processes involving non-covalent protein immobilization in chromatography resins at high temperatures. Therefore, we checked the thermal stability of C-LytA and C-LytAm7 when bound to a DEAE-cellulose affinity chromatography. After a 30 min incubation at different temperatures, the amount of functional protein (i.e. able to bind choline) was measured upon elution with the ligand at room temperature. As shown in Fig. 7, the midpoint of the C-LytA denaturation curve can be calculated at ~62°C. It is noteworthy that a significant 30% of protein retained its functionality even after incubation at 90°C. On the other hand, the C-LytAm7 protein maintains a substantial 85% of functional molecules after a high temperature treatment (Fig. 7). This can be useful in biotechnological procedures requiring, for example, the previous sterilization step of a bioreactor. However, it can be argued that a certain population of C-LytAm7 molecules might yet be unfolded at high temperatures but recover their choline-recognition ability after the re-equalibration step prior to elution. Therefore, the differences found in the percentage of protein eluted by choline would be a consequence of the higher reversibility of C-LytAm7 denaturation rather than due to the amplification of the mutant stabilization by interaction with the chromatographic matrix. To verify the actual state of the proteins at high temperatures, we performed a variant of the experiment at 70°C omitting the re-equilibration step and carrying out the elution at the same temperature. Yields were 18% for wild-type and 72% for the thermostable mutant, in the same range as the data shown in Fig. 7. This confirms that the moderate increase in thermostability displayed by the choline-bound form of the mutant in solution (7°C) is then widely amplified within the chromatographic matrix. All these data therefore confirms that C-LytAm7 may be used as an efficient alternative to the wild-type C-LytA affinity tag in biotechnological processes requiring high temperatures.

Effect of acidic pH The application of wild-type C-LytA as an affinity tag is currently reduced to a pH around neutrality. The reason for this is the low solubility of the protein at acidic pHs. This is clearly shown in Fig. 8A, which displays the pH dependence of the ellipticity value at 223 nm. The signal is unaltered between pH 6.5 and 10.7 and decreases below pH 6.0 and above pH 10.7, in the latter case as a consequence of protein denaturation (Fig. 8B). There is a minimum between pH 4.5 and 5.5, where the CD signal is barely detectable. The CD spectrum registered at pH 5.0

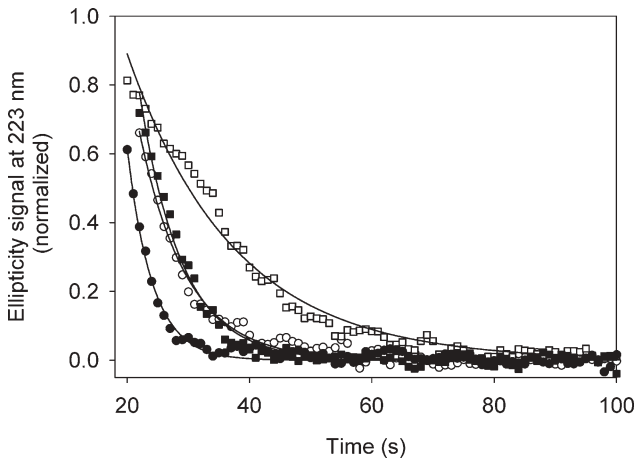

Fig. 6. Temperature-induced unfolding kinetics. Open circle, C-LytA at 70°C; open box, C-LytAm7 at 70°C; filled circle, C-LytA at 80°C in the presence of 10 mM choline; filled box, C-LytAm7 at 80°C in the presence of 10 mM choline.

Table IV. Kinetic stability of C-LytA and C-LytAm7

Protein	Unfolding rate constants (s^{-1})	
	No choline (70°C)	10 mM choline (80°C)
C-LytA	0.13 ± 0.01	0.25 ± 0.01
C-LytAm7	0.06 ± 0.01	0.14 ± 0.01

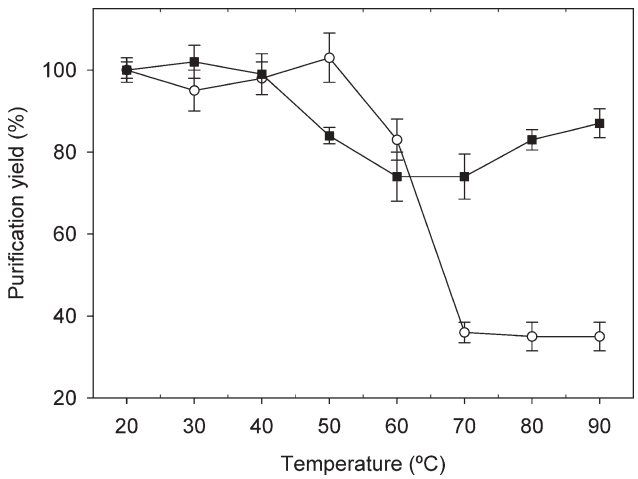

Fig. 7. Effect of temperature on the stability of C-LytA and C-LytAm7 bound to DEAE-cellulose. Proteins were eluted from a DEAE-cellulose column after a 30 min incubation at different temperatures. Results are the average of two independent experiments. Open circle, C-LytA; filled box, C-LytAm7.

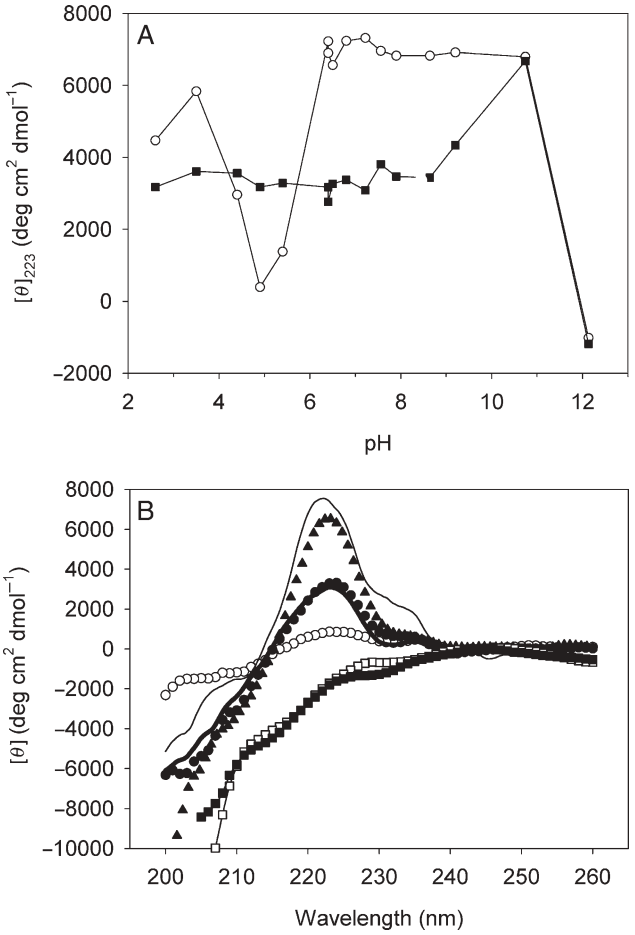

Fig. 8. Effect of pH on the far-UV CD of C-LytA and C-LytAm7 at 20°C. (A) Ellipticity at 223 nm as a function of pH: open circle, C-LytA; filled box, C-LytAm7. (B) Wavelength scans: C-LytA at pH 7.0 (solid line), pH 5.0 (open circle) and pH 12.2 (open box), and C-LytAm7 at pH 7.0 (thick solid line), pH 5.0 (filled circle), pH 10.7 (filled triangle) and pH 12.2 (filled box).

(Fig. 8B) shows a general decrease in the signal at all wavelengths, concomitant with a reduced absorbance of the sample (data not shown). This fact suggests that the solubility of C-LytA is minimal around this pH, causing protein aggregation and leading to a decreased population of soluble molecules susceptible of yielding a CD spectrum. On the other hand, the introduction of five net positive charges in C-LytAm7 improved the solubility in a wider pH range (Fig. 8A). Figure 8B also shows that the wavelength spectrum of C-LytAm7 at pH 5.0 is undistinguishable from that recorded at pH 7.0, confirming the presence of native structure in these conditions. Remarkably, there is a clear increase in CD signal at pH 10.7, preceding the protein denaturation at higher pHs. The spectrum of C-LytAm7 registered at this pH resembles that of the wild-type form (Fig. 8B). This phenomenon reminds that displayed in Figs 2B and 4B, where the addition of NaCl also induces an enhancement of the CD spectrum of the mutant. We are tempted to speculate that, as a consequence of the introduction of a certain lysine residue by mutation, a particular electrostatic interaction might affect locally the environment of some aromatic residues in the protein, causing a decrease in the CD signal. Therefore, screening of this interaction by salt, or its removal by lysine deprotonation at alkaline pH, would restore the native CD spectrum.

The results depicted in Fig. 8A demonstrate that C-LytAm7 has a potentially wider range of applications than its wild-type counterpart with respect to working pH. We considered of interest to check whether this general solubilization of C-LytAm7, and in particular at low pHs, could also be useful for the immobilization and purification of proteins in acidic conditions. To do so, we carried out a standard purification experiment in which the pH was set to 5.0 in all steps (immobilization, washing and elution). As expected, the yield of wild-type C-LytA was low (7% compared with pH 7.0), but that of C-LytAm7 increased to a remarkable 40%, taking into account that the protein is positively charged at pH 5.0 to a great extent (around +10), so that the electrostatic repulsions with the DEAE groups in the column strongly compete with the affinity for the diethylaminoethyl group.

Concluding remarks: biotechnological potential of the C-LytAm7 tag

The properties of C-LytA make it an attractive tag for the non-covalent immobilization and purification of proteins. Therefore, we decided to use protein engineering procedures in order to strengthen its stability and widen its application landscape. The work presented here shows how the engineering of surface ionic networks can significantly improve the thermal stability and biotechnological performance of the C-LytA affinity tag, confirming that the creation of surface salt bridges constitutes an appealing method that may be considered as a valid choice for the thermal stabilization of proteins. In particular, the introduction of seven surface mutations in the protein, leading to the C-LytAm7 mutant, caused a moderate thermal stabilization of the tag. Nevertheless, the most remarkable results are the suppression of folding intermediates, a complete reversibility upon thermal denaturation and a decreased kinetic rate on thermal unfolding. Moreover, the mutations greatly improved the solubility and stability of the protein in a wide pH range, both in solution and attached to the column, broadening the potential application of this tag for protein purification in acidic conditions. In comparison, immobilized metal affinity chromatography, which makes use of histidine tags, can only be employed at pHs >6.5 for the histidines to be deprotonated and to effectively interact with the metal-containing support (Gaberc-Porekar and Menart, 2001), and purifications using the maltose-binding protein and glutathione-*S*-transferase are also reported only at neutral pHs (Terpe, 2003). In conclusion, the C-LytAm7 mutant represents a much improved binding of the tag to its affinity column at high temperatures and low pHs and paves the way for the purification of recombinant proteins and the operation of thermostable enzyme bioreactors under far-from-standard conditions.

Funding

Spanish Ministerio de Educación y Ciencia (MEC) [CIT-010000-2005-32, FIT-010000-2003-110], Fundación SALVAT-Inquifarma.

Acknowledgements

We are greatly indebted to Professor Javier Gómez for invaluable help in interpreting the thermal denaturation data. We would also like to thank

I. Castillejo, C. Fuster and A. Rodríguez for excellent technical assistance. V.M.H.-R. is a recipient of a Formación de Personal Universitario fellowship from Spanish Ministerio de Educación y Ciencia (MEC).

References

Akerström,B., Lögdberg,L., Berggård,T., Osmark,P. and Lindqvist,A. (2000) *Biochim. Biophys. Acta*, **1482**, 172–184.
Backmann,J., Schäfer,G., Wyns,L. and Bönisch,H. (1998) *J. Mol. Biol.*, **284**, 817–833.
Baldwin,R.L. and Eisenberg,D. (1987) In Oxender,D.L. and Fox,C.F. (eds), *Protein Engineering*. Alan R. Liss, New York, pp. 127–148.
Bernstein,H.J. (2000) *Trends Biochem. Sci.*, **25**, 453–455.
Biomedal,S.L. (2004), http://www.biomedal.es.
Caubin,J., Martin,H., Roa,A., Cosano,I., Pozuelo,M., de la Fuente,J.M., Sánchez-Puelles,J.M., Molina,M. and Nombela,C. (2001) *Biotechnol. Bioeng.*, **74**, 164–171.
Cheung,Y.Y., Lam,S.Y., Chu,W.K., Allen,M.D., Bycroft,M. and Wong,K.B. (2005) *Biochemistry*, **44**, 4601–4611.
Elcock,A.H. (1998) *J. Mol. Biol.*, **284**, 489–502.
Fernández-Tornero,C., López,R., García,E., Giménez-Gallego,G. and Romero,A. (2001) *Nat. Struct. Biol.*, **8**, 1020–1024.
Freire,E., Luque,I. and Townsend,B. (1997) *ASAcalc: Calculation of Accessible Surface Areas, v. 1.0.* Biocalorimetry Center, The Johns Hopkins University.
Gaberc-Porekar,V. and Menart,V. (2001) *J. Biochem. Biophys. Methods*, **49**, 335–360.
Greene,R.F., Jr and Pace,C.N. (1974) *J. Biol. Chem.*, **249**, 5388–5393.
Guex,N. and Peitsch,M.C. (1997) *Electrophoresis*, **18**, 2714–2723.
Iqbalsyah,T.M. and Doig,A.J. (2005) *Biochemistry*, **44**, 10449–10456.
Karshikoff,A. and Ladenstein,R. (2001) *Trends Biochem. Sci.*, **26**, 550–556.
Kirk,O., Borchert,T.V. and Fuglsang,C.C. (2002) *Curr. Opin. Biotechnol.*, **13**, 345–351.
Knapp,S., de Vos,W.M., Rice,D. and Ladenstein,R. (1997) *J. Mol. Biol.*, **267**, 916–932.
Lee,B. and Richards,F.M. (1971) *J. Mol. Biol.*, **55**, 379–380.
Loladze,V.V., Ibarra-Molero,B., Sánchez-Ruiz,J.M. and Makhatadze,G.I. (1999) *Biochemistry*, **38**, 16419–16423.
Maes,D., *et al*. (1999) *Proteins*, **3**, 441–453.
Maestro,B. and Sanz,J.M. (2005) *Biochem. J.*, **387**, 479–488.
Maestro,B. and Sanz,J.M. (2007) *FEBS Lett.*, **581**, 375–381.
Maestro,B., González,A., García,P. and Sanz,J.M. (2007) *FEBS J.*, **274**, 364–376.
Makhatadze,G.I., Loladze,V.V., Ermolenko,D.N., Chen,X.F. and Thomas,S.T. (2003) *J. Mol. Biol.*, **327**, 1135–1148.
Medrano,F.J., Gasset,M., López-Zúmel,C., Usobiaga,P., García,J.L. and Menéndez,M. (1996) *J. Biol. Chem.*, **271**, 29152–29161.
Moldes,C., García,J.L. and García,P. (2004) *Appl. Environ. Microbiol.*, **70**, 4642–4647.
Myers,J.K., Pace,C.N. and Scholtz,J.M. (1995) *Protein Sci.*, **4**, 2138–2148.
Nelson,D., Loomis,L. and Fischetti,V.A. (2001) *Proc. Natl Acad. Sci. USA*, **98**, 4107–4112.
Numata,K., Muro,M., Akutsu,N., Nosoh,Y., Yamagishi,A. and Oshima,T. (1995) *Protein Eng.*, **8**, 39–43.
Ortega,S., García,J.L., Zazo,M., Varela,J., Muñoz-Willery,I., Cuevas,P. and Giménez-Gallego,G. (1992) *Biol. Technol.*, **10**, 795–798.
Pérez-Jiménez,R., Godoy-Ruiz,R., Ibarra-Molero,B. and Sánchez-Ruiz,J.M. (2005) *Biophys. Chem.*, **115**, 105–107.
Petsko,G.A. (2001) *Methods Enzymol.*, **334**, 469–478.
Ruíz-Echevarría,M.J., Giménez-Gallego,G., Sabariegos-Jareño,R. and Díaz-Orejas,R. (1995) *J. Mol. Biol.*, **247**, 568–577.
Sánchez-Puelles,J.M., Sanz,J.M., García,J.L. and García,E. (1990) *Gene*, **89**, 69–75.
Sánchez-Puelles,J.M., Sanz,J.M., García,J.L. and García,E. (1992) *Eur. J. Biochem.*, **203**, 153–159.
Sanz,J.M., López,R. and García,J.L. (1988) *FEBS Lett.*, **232**, 308–312.
Strickler,S.S., Gribenko,A.V., Gribenko,A.V., Keiffer,T.R., Tomlinson,J., Reihle,T., Loladze,V.V. and Makhatadze,G.I. (2006) *Biochemistry*, **45**, 2761–2766.
Swint,L. and Robertson,A.D. (1993) *Prot. Sci.*, **2**, 2037–2049.
Tahirov,T.H., Oki,H., Tsukihara,T., Ogasahara,K., Yutani,K., Ogata,K., Izu,Y., Tsunasawa,S. and Kato,I. (1998) *J. Mol. Biol.*, **284**, 101–124.
Tanner,J.J., Hecht,R.M. and Krause,K.L. (1996) *Biochemistry*, **35**, 2597–2609.
Terpe,K. (2003) *Appl. Microbiol. Biotechnol.*, **60**, 523–533.
Uhlen,M., Forsberg,G., Moks,T., Hartmanis,M. and Nilsson,B. (1992) *Curr. Opin. Biotechnol.*, **3**, 363–369.
Unsworth,L.D., van der Oost,J. and Koutsopoulos,S. (2007) *FEBS J.*, **274**, 4044–4056.
Usobiaga,P., Medrano,F.J., Gasset,M., García,J.L., Saiz,J.L., Rivas,G., Laynez,J. and Menéndez,M. (1996) *J. Biol. Chem.*, **271**, 6832–6838.
van den Burg,B. and Eijsink,V.G. (2002) *Curr. Opin. Biotechnol.*, **13**, 333–337.
Vieille,C. and Zeikus,G.J. (2001) *Microbiol. Mol. Biol. Rev.*, **65**, 1–43.
Waugh,D.S. (2005) *Trends Biotechnol.*, **23**, 316–320.
Yip,K.S., *et al*. (1995) *Structure*, **3**, 1147–1158.

Received February 14, 2008; revised July 21, 2008; accepted August 6, 2008

Edited by Jane Clarke